NJC

RSC Publishing

PAPER

View Article Online
View Journal

Cite this: DOI: 10.1039/c3nj00371j

Tuning of the H-bonding ability of imidazole N–H towards the colorimetric sensing of fluoride and cyanide ions as their sodium salts in water†

Ramalingam Manivannan, Angupillai Satheshkumar and Kuppanagounder P. Elango*

Received (in Montpellier, France)
9th April 2013,
Accepted 8th July 2013

DOI: 10.1039/c3nj00371j

www.rsc.org/njc

Imidazole functionalized receptors, 2-*R*-1*H*-naphtho[2,3-*d*]imidazole-4,9-dione (**2a–h**), containing naphthoquinone as a chromogenic signalling unit have been synthesized from the reaction of 2,3-diaminonaphthoquinone and different aldehydes. These receptors showed a color change upon addition of fluoride and cyanide ions in DMSO with a bathochromic shift of the characteristic intramolecular charge transfer (ICT) transition band. No color change was observed upon addition of other anions such as Cl^-, Br^-, I^-, NO_3^-, AcO^- and $H_2PO_4^-$. ^1H NMR and electrochemical studies revealed that these receptors sense fluoride and cyanide ion *via* the formation of H-bond with the imidazole N–H moiety. Electronic and spectrofluorimetric studies indicated that the binding constants of these receptors with F^- and CN^- ions were in the order of $\sim 10^6$. The results of the spectral studies indicated that, by changing the R group in the receptor, the acidity of the imidazole N–H can be varied from δ_H 13.70 (for isopropyl) to 14.94 ppm (for thiophene). Theoretical calculations based on Density Functional Theory showed that the HOMO–LUMO energy gap for the ICT transition corroborate the results of the spectral studies. Receptor **2f** (R = thiophene) was also able to detect fluoride and cyanide ions as their sodium salts in aqueous solution with a visual color change.

Introduction

The development of molecular sensors for anions is receiving increased attention due to their significant roles in biology, medicine, catalysis and environmental monitoring.[1–4] Anions, particularly fluoride, cyanide and phosphate, are harmful to environment as well as human health.[5–7] According to the World Health Organization (WHO), the permissible limit of fluoride and cyanide ion concentrations in drinking water is 1.5 and 0.07 mg L^{-1}, respectively.[8,9] Consequently, the selective detection of these anions, either visually or by spectroscopic/electrochemical methods, has become essential. Moreover, single molecular sensors for multiple analytes have become a new research focus because it could overcome the difficulties encountered with loading multiple indicators.[10–12]

In general, molecular sensors are composed of two units: receptor and signalling units.[13,14] A survey of the literature revealed that various authors have developed molecular sensors containing urea/thiourea,[15,16] pyrrole,[17,18] indole,[19,20] imidazole,[21,22] calyx[23] and calixarenes[24] as the receptor units due to their H-bond donor properties. Moieties such as nitrophenyl,[25,26] quinone[27,28] and azo-dye[29–31] were used as signalling units in these sensors. Recently, we developed a molecular sensor based on urea for the simple and selective detection of fluoride ions, where the receptor unit is directly attached to the quinone signalling unit in order to achieve a receptor unit with an enhanced H-bond donor property,[14] as the anion recognition event solely depends on the H-bonding property of the sensors.

Recently, we have demonstrated the intermolecular charge transfer facilitated imine formation of a weak nucleophile, 2,3-diaminonaphthoquinone (**I**) with different aldehydes.[32] Spectroscopic and theoretical studies revealed that the weak nature of these amine groups is due to the existence of an intramolecular charge transfer (ICT) transition between the amine and quinone moieties. Such an ICT transition would increase the H-bond donor ability (acidity) of the amine group. Also in the imine (**II**) obtained from the amine, the acidity of the H-atoms were found to be increased as a result of unequal ICT transition from the two substituents attached to the quinone ring. The results of the study also revealed that the ICT from the amine nitrogen in **II** is relatively higher than from the imine nitrogen.

Hence, it was presumed that by attaching an imidazole moiety (which already possesses an acidic H-atom) directly to

Department of Chemistry, Gandhigram Rural Institute (Deemed University), Gandhigram 624 302, India. E-mail: drkpelango@rediffmail.com; Fax: +91 451 2454466

† Electronic supplementary information (ESI) available: UV-Vis and fluorescence titration, optimized structure HOMO–LUMO Structure and ^1H, ^{13}C NMR and LCMS spectra of all products. See DOI: 10.1039/c3nj00371j

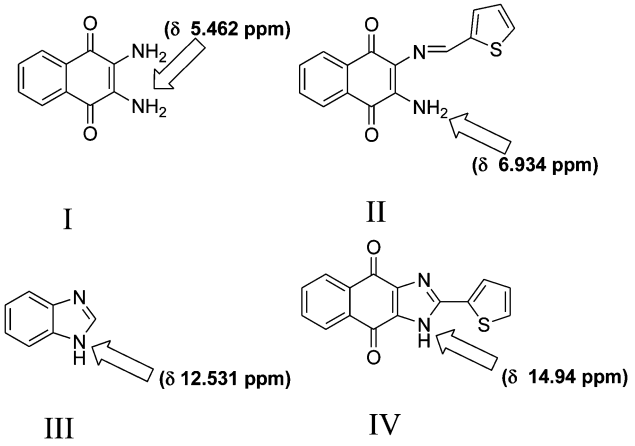

the quinone ring, we could enhance the acidity of the imidazole H-atom (**IV**).Also, by varying the substituent attached to the imidazole ring we could fine tune the H-bond donor ability of the N–H group of such an imidazole system. Further, when the receptor unit (imidazole moiety) is directly attached to the signalling unit (quinone moiety), the ICT transition would be more pronounced so as to make its detection easier. Furthermore, such structural variation can also alter the solubility of the molecule.[33]

The main objective, therefore, of the present endeavour is to synthesize a series of such imidazoles (**IV**) with varying substituents and to make use of these molecules as sensors for anions. The interaction between the sensors and anions was investigated using various spectral (UV-Vis, fluorescence, ^{1}H NMR) and electrochemical studies. For better understanding of the sensing behaviors, the structures and electronic properties of the sensors and their complexes with fluoride and cyanide ions have also been calculated using Density Functional Theory.

Result and discussion

Receptors **2a–h** were synthesized, from commercially available 2,3-dichloronaphthoquinone, as outlined in Scheme 1. The structure of these compounds was characterized by ^{1}H NMR, LCMS and UV-Vis spectral techniques. All the compounds synthesized (except **2a**) are novel. The anion recognition property of these receptors was investigated using various spectral techniques such as UV-Vis, fluorescence and ^{1}H NMR and DFT computations.

Visual detection

Visual inspection of compounds **2a–h** (6.25×10^{-4} M) in DMSO before and after addition of 1 eq. of tetrabutylammonium salts of various anions, such as F^-, CN^-, Cl^-, Br^-, I^-, AcO^-, $H_2PO_4^-$ and NO_3^-, was carried out. As a representative case, the color change observed for **2f** is shown in Fig. 1. As depicted in the figure, the DMSO solution of **2f** turned yellow to intense red after the addition of fluoride and cyanide ions. However, the color remained unchanged after the addition of the other

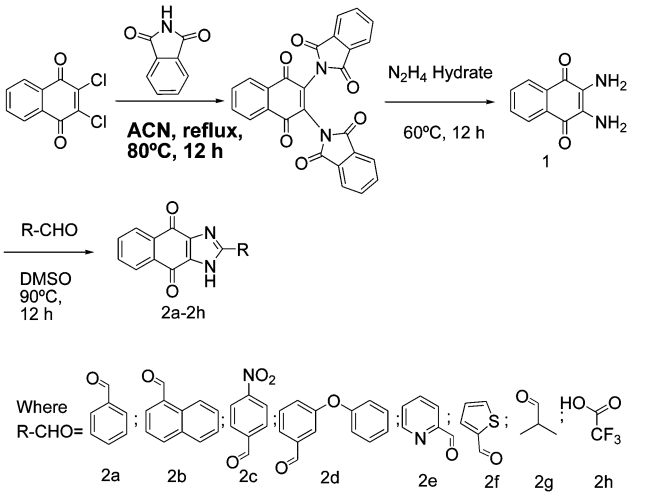

Scheme 1 Synthesis of receptors **2a–h**.

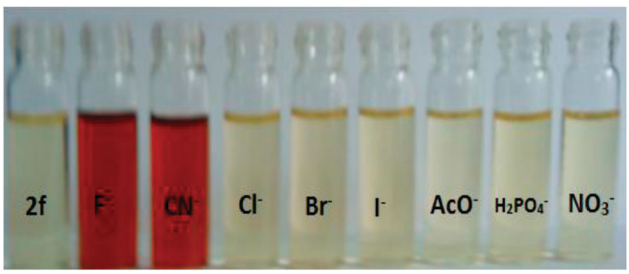

Fig. 1 Color changes upon addition of (1 eq.) of various anions to DMSO solutions of **2f** (6.25×10^{-4} M).

chosen anions. This observation indicated the selectivity of **2a–h** toward fluoride and cyanide ions.[34]

Binding studies using UV-Vis spectrophotometry

The complexation abilities of **2a–h** with these anions were investigated using an UV-Vis absorption technique. As a representative case, the UV-Vis spectral changes of **2f** upon the addition of the different anions are shown in Fig. 2. The electronic spectrum of receptor **2f** exhibited a maximum absorbance at 428 nm (log ε = 5.83), which corresponds to the intramolecular charge transfer (ICT) transition (n $\rightarrow$ π^*) from N-atoms to the quinone moiety. As evidenced from Fig. 2, the addition of fluoride and cyanide ions bathochromically shifts the λ_{ICT} to 486 nm, which is accompanied by the instantaneous formation of the red color ($\Delta\lambda_{ICT}$ = 58 nm). However, addition of other anions produced only a very small shift in the λ_{ICT}. With the addition of incremental amounts of fluoride and cyanide ions to the solution of **2f** in DMSO–HEPES buffer (1 : 1 v/v),[35–41] the absorption peak at 424 nm diminished gradually while the formation of a new peak at 485 nm was observed (Fig. 3). This new band is due to the ICT transition between the receptor (imidazole N–H$\cdots$A$^-$; where A$^-$ = F$^-$ or CN$^-$) and quinone signalling units. Thus, the bathochromic

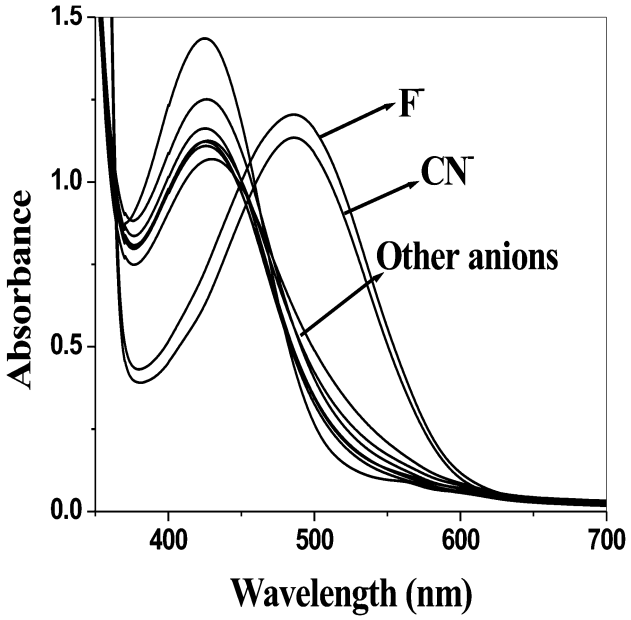

Fig. 2 UV-Vis absorption changes of compound **2f** (6.25×10^{-4} M) upon addition of 1 eq. of $[(Bu)_4N]$ salts of F^-, CN^-, Cl^-, Br^-, I^-, AcO^-, NO_3^-, $H_2PO_4^-$ in DMSO.

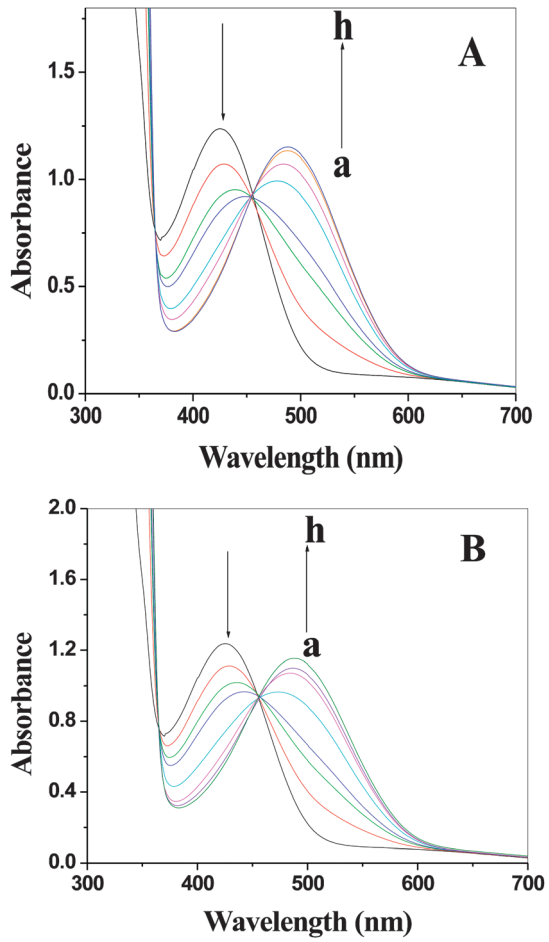

Fig. 3 Change in UV-Vis spectra for **2f** (6.25×10^{-4} M) in 1 : 1 DMSO–HEPES buffer (0.1 M, pH 7.4) (A) with the addition of [0 (a)–(h) 6.25×10^{-4} M] of fluoride ions, (B) with the addition of [0 (a)–(h) 6.25×10^{-4} M] cyanide ions.

Table 1 Association and binding constants (K_A) of **2a–2h** interaction with F^- and CN^-

	Association constant $(K_d)^a/M^{-1}$		Binding constant $(K_A)^b/mol^{-1}$ L	
Receptor	F^-	CN^-	F^-	CN^-
2a	2.4×10^5	2.9×10^4	4.5×10^5	1.6×10^4
2b	3.1×10^5	3.9×10^5	8.7×10^5	1.4×10^5
2c	1.5×10^5	1.3×10^5	4.9×10^6	4.1×10^6
2d	1.2×10^5	9.7×10^4	3.2×10^5	1.8×10^5
2e	3.7×10^5	5.8×10^4	3.4×10^6	7.7×10^5
2f	3.2×10^6	2.6×10^6	7.2×10^6	7.0×10^6
2g	2.9×10^4	2.4×10^4	6.4×10^3	5.9×10^3
2h	1.1×10^5	7.7×10^4	9.6×10^5	4.4×10^5

[a] From the Scott linear plot (UV-Vis titration method). [b] From the Ward method (fluorescence quenching study).

shift observed in the λ_{ICT}, upon addition of F^- and CN^- ions, is due to the fact that the N–H···A^- unit is a relatively better electron donor than the free imidazole N–H group in the ICT transition.[14,34]

The isosbestic point (at 455 nm) indicated that only one type of receptor–A^- complex exists.[34,42] All other receptors produced similar UV-Vis spectral changes (Fig. S1 and S2, ESI†). In all cases, the association constant of the receptor–A^- complex was determined from the linear ($r > 0.96$) Scott plots[43] and are collected in Table 1. The results in Table 1 indicate that receptor **2f** has significantly large association constants (in the order of 10^6 M^{-1}) for fluoride and cyanide ions. Interestingly, the receptor **2f** exhibited similar electronic spectral changes in a 1 : 1 v/v DMSO–water mixture also. Such an observation indicated that receptor **2f** can form a receptor–A^- complex in an aqueous medium also. The electronic spectra of **2f** were also recorded in DMSO–water mixtures of varying compositions (Fig. S3, ESI†). As expected, the results showed that when the water content of the medium increased, there was a decrease in the absorbance of the solution with a concurrent blue shift in the absorption maximum.

Binding studies using fluorescence spectrophotometry

The anion binding ability of the receptors **2a–h** was also evaluated by fluorescence titration studies. The fluorescence emission spectra of the receptors (6.25×10^{-4} M) showed a broad peak around 530 nm when excited at the corresponding λ_{ICT}. In all cases, upon gradual addition of fluoride (Fig. 4) and cyanide (Fig. S4, ESI†) ions to the receptor solution, quenching of fluorescence was observed, indicating complexation between the receptors and fluoride/cyanide ions. From the decrease in the emission intensity, the binding constant of the receptor–A^- complex was calculated using the following equation,[14,44]

$$\log(F_0 - F)/F = \log K_A + n \log[Q]$$

where F_0 is the emission intensity in the absence of quencher (Q), F is the emission intensity at the quencher concentration $[Q]$ and K_A is the binding constant for the receptor–A^- complex. In all the cases, a plot of $\log(F_0 - F)$ *versus* $\log[Q]$ is linear

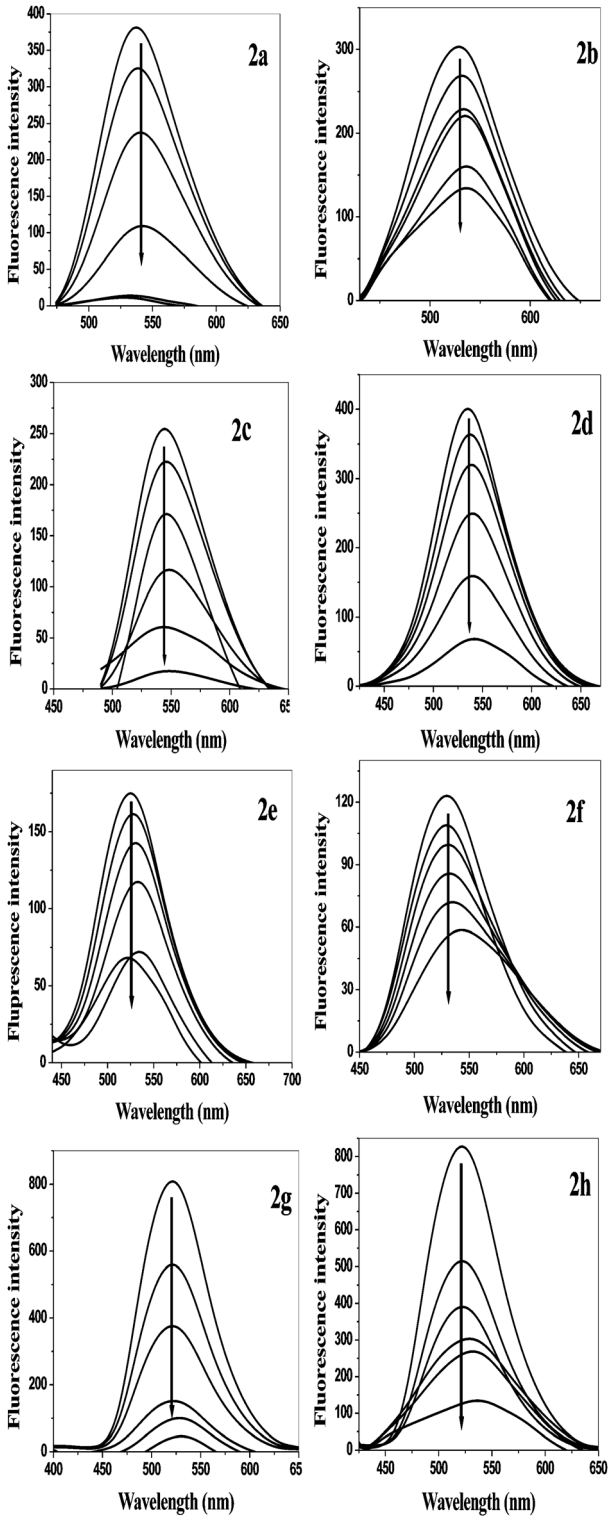

Fig. 4 Change in fluorescence emission spectra for **2a–h** (6.25×10^{-4} M) in DMSO upon the addition of $[(Bu)_4N]F$ in DMSO from 0–6.25×10^{-4} M.

($r > 0.95$) and the binding constants thus determined are also collected in Table 1.

The results indicated that the K_A values depend on the substituents present in the receptor. However, as no quantitative correlation between the K_A values and R have been made at present, we will reserve the discussion for a while.

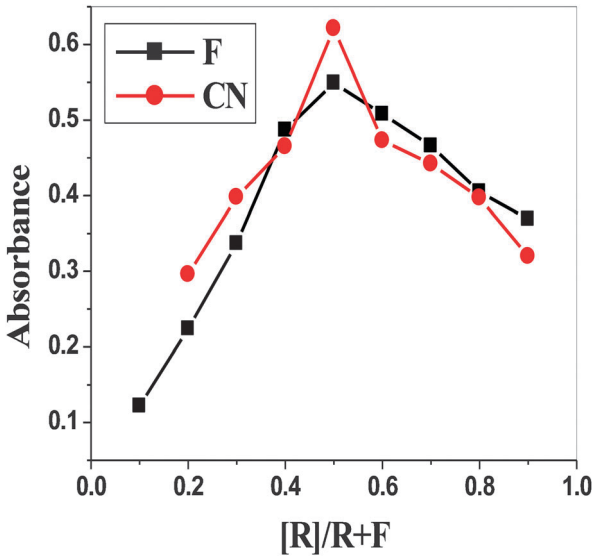

Fig. 5 The stoichiometry analysis of **2f** by Job's plot with F^- and CN^-.

The stoichiometry of the interaction between the receptors and A^- was determined using the UV-Vis spectral data.[45] A representative Job's plots for **2f–F**$^-$ and **2f–CN**$^-$ are shown in Fig. 5. A curve with a maximum at 0.5 mole fraction was observed in both the cases, indicating the formation of 1 : 1 (receptor : A^-) complex.[45]

^{1}H NMR titration studies

^{1}H NMR titration experiments were performed to understand the character of the receptor–anion interactions. As a representative case, the ^{1}H NMR spectra, recorded in DMSO-d_6, of receptor **2f** in the absence and presence of fluoride ions are shown in Fig. 6. All other ^{1}H NMR spectra are given in the ESI.† The ^{1}H NMR spectrum of **2f** showed a singlet at δ 14.94 ppm for the imidazole N–H proton.

Upon the addition of incremental amounts of fluoride ions, the ^{1}H NMR peak of the imidazole N–H proton of these receptors (**2a–h**) moved down field and then disappeared after the addition of 1 eq. of F^- ions.[46] While in the case of CN^-, there was an up field shift of the NH proton, which falls in the shielding zone of the ring current of the triple bond of the CN^- ion. However, no noticeable changes were observed in the NMR peaks of other protons. These results indicated that the electrostatic interactions between the imidazole N–H of these receptors and the fluoride/cyanide ions occur without any redistribution of the electron cloud. Therefore, the color change can be attributed to the formation of H-bonding between the imidazole N–H of these receptors and the fluoride/cyanide ions.[34,46] As we presumed in the introduction section, the imidazole N–H proton in these receptors are more acidic than that of benzimidazole itself. This may be due to the fact that, in the present cases **2a–h**, the imidazole receptor unit is directly attached to an electron deficient

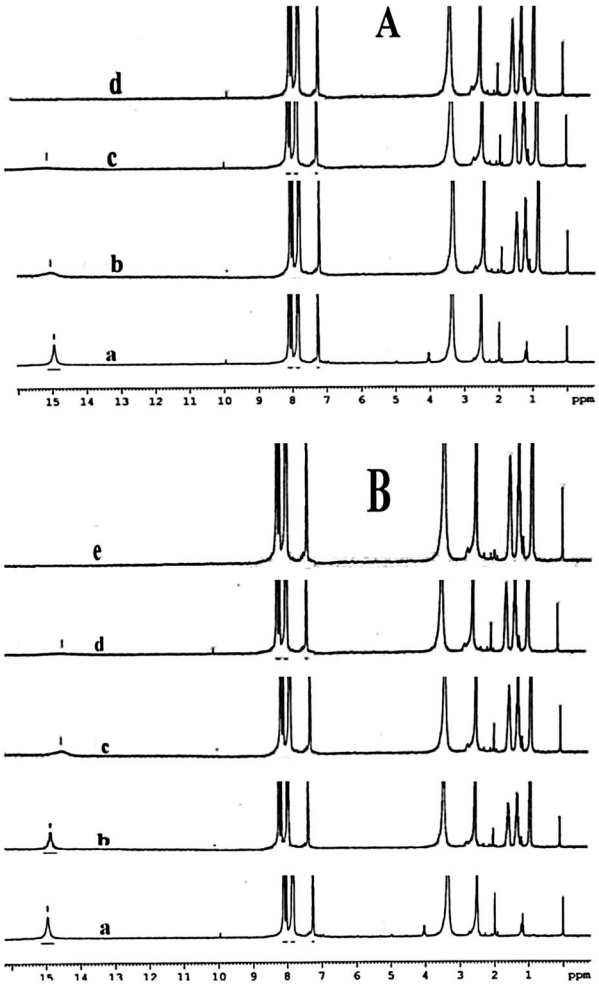

Fig. 6 (A) Partial NMR spectrum of **2f**: with (a) 0.25, (b) 0.5, (c) 0.75 and (d) 1.0 eq. of F^- in DMSO-d_6. (B) Partial NMR spectrum of **2f**: with (a) 0.25, (b) 0.5, (c) 0.75, (d) 1.0 and (e) 2.0 eq. of CN^- in DMSO-d_6.

quinone signalling unit, where the ICT transition existing between these two units make the N–H proton more acidic. Also, by varying the substituent (R) attached to the imidazole ring, the acidity of the N–H proton can be fine-tuned (Table 2). In the present study the highest δ = 14.94 ppm was observed with thiophene substituted imidazole and the lowest δ = 13.70 ppm was observed for the isopropyl substituted compound. Since the mechanism of sensing of fluoride and cyanide ions by these

Table 2 Selected spectral and theoretical data of the receptors

		Receptor		Receptor–F		Receptor–CN	
Entry	δ(NH)	λ_{max}	ΔE	λ_{max}	ΔE	λ_{max}	ΔE
2a	14.37	414.0	3.3699	479.0	2.0382	478.0	2.4011
2b	14.41	416.0	3.0384	476.0	2.0487	476.0	1.8659
2c	14.89	377.0	3.5783	442.0	2.2123	442.0	2.2259
2d	14.39	404.5	3.1876	469.0	1.2025	469.0	1.4759
2e	14.62	385.0	3.6173	459.0	3.5696	458.5	3.0896
2f	14.94	428.5	3.2044	485.0	2.3870	486.0	2.4585
2g	13.70	389.5	3.8807	461.0	2.3407	461.0	2.8634
2h	14.63	355.5	4.0306	404.5	3.2996	404.0	3.4523

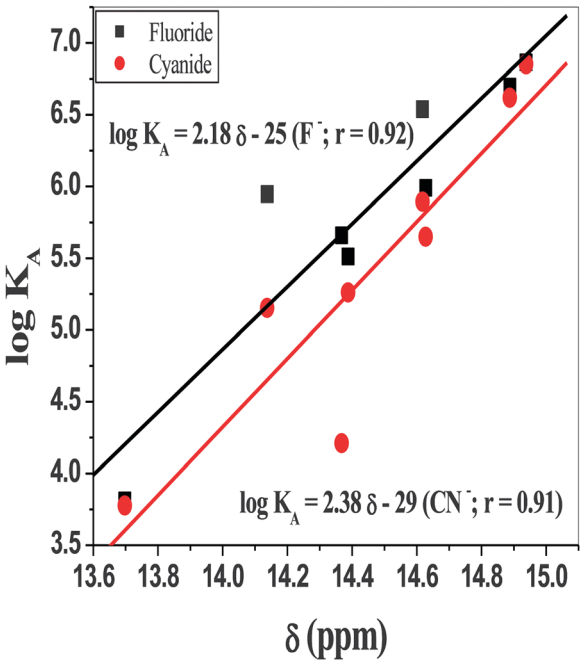

Fig. 7 Correlation between association constants (K_A) and chemical shifts (δ_H).

receptors involves the formation of H-bonds between the imidazole N–H moiety and the anions, the acidity of the N–H protons would alter the strength of the H-bonds. Interestingly, there exists a fairly linear correlation ($r > 0.91$) between the logK_A and δ values (Fig. 7), with positive slopes observed for both fluoride and cyanide ion sensing. The positive slopes indicated that an increase in the acidity of the imidazole N–H proton increases the magnitude of the binding constant of the receptor–A^- complex.

Electro-chemical studies

One interesting attribute of the receptors **2a–h** is the attachment of the anion binding site (imidazole N–H moiety) directly to the redox-active quinone moiety. As a representative case, the electrochemical properties of receptor **2f**, on its own as well as in the presence of variable concentrations of fluoride and cyanide ions, were investigated using a Differential Pulse Voltammetry (DPV) technique in DMSO. Since the redox couples in the presence of anions could not be discerned by cyclic voltammetry, these were also measured using the more sensitive DPV technique. The DP voltammograms are shown in Fig. 8. The receptor **2f** showed two reduction peaks, which is the typical behavior of a quinone. The first peak (−0.1003 V) corresponds to the formation of the radical anion ($Q^{\cdot-}$) and the second peak at a relatively more negative potential (−0.5457 V) corresponds to the formation of the dianion (Q^{2-}). In traditional organic solvents the difference in these two peak potentials approaches a few hundred millivolts[47] and in the present study it is 445 mV.

The results depicted in Fig. 8 indicate that on the addition of incremental amounts of these anions (F^- and CN^-) the current intensities of the two reduction peaks decreased with

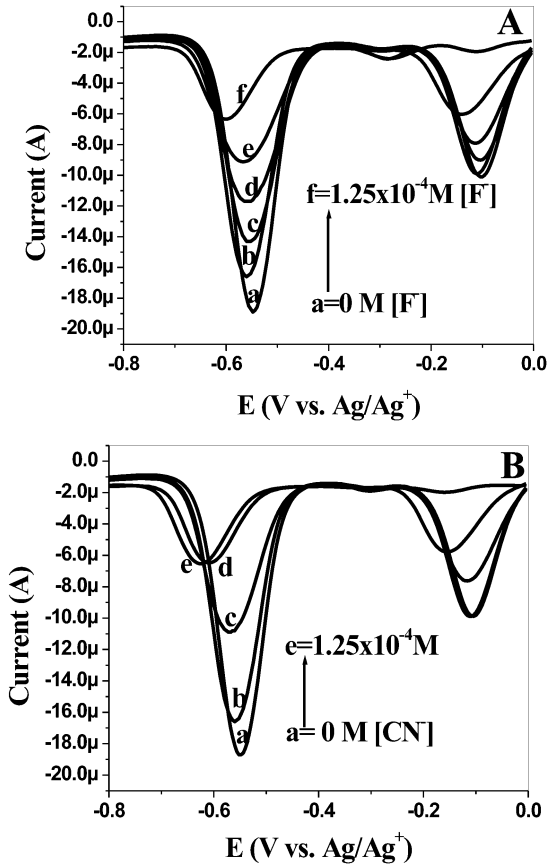

Fig. 8 Changes in redox properties of **2f** (1 mM) in DMSO upon addition of (A) $[(Bu)_4N]F$ in DMSO from 0–1.25 × 10^{-4} M, (B) $[(Bu)_4N]CN$ in DMSO from 0–1.25 × 10^{-4} M.

a concomitant shift of the peaks to a more negative potential. That is, the addition of these anions made the electro-reduction of the quinone relatively more difficult.[21,28]

This may be due to the fact that complexation of these anions with the imidazole N–H moiety, through H-bonding, makes the N-atom relatively electron rich and thus increases the intensity of ICT transition (from N–H to quinone) and consequently renders the quinone difficult to reduce. In other words, the N–H···A^- moiety is a relatively better electron donor than the free N–H group in the ICT transition. The results corroborate the observations made in the electronic spectral studies, wherein the addition of these anions to the receptors bathochromically shifts the ICT peak.

Theoretical studies

The structural and electronic properties of the receptors **2a–h** and their complexes with fluoride and cyanide ions were investigated, using Density Functional Theory calculations, with an aim to elaborate the mechanism of the anion recognition abilities of these receptors. The geometry optimizations were carried out using the B3LYP exchange functional with 6311G basis sets from the Gaussian 03 package.[48] All the optimized geometries are shown in Fig. S4 (ESI†). The relevant frontier molecular orbitals (HOMO and LUMO) of **2a–h** and their complexes with F^- and CN^- ions are shown in Fig. S5–S7 (ESI†). As shown in Fig. S5–S7 (ESI†), in these receptors the HOMO distribution is concentrated on the imidazole ring and the LUMO is concentrated on the quinone moiety, as expected. In **2a–h**, the electronic transition from the HOMO to LUMO is responsible for the ICT transition observed around 400 nm in the UV-Vis spectra. The energy corresponding to the ICT transition ($\Delta E = E_{HOMO} - E_{LUMO}$) along with λ_{ICT} are collected in Table 2. In these cases, there exists a fairly linear correlation ($r \sim 0.9$) between λ_{ICT} and ΔE, with a negative slope, as expected. The complexation of F^- or CN^- ions with the receptors decreased the ΔE value, red shifted the λ_{ICT} and consequently makes the colorimetric recognition of these ions energetically easier. This is due to the fact that the N–H···A^- moiety is a relatively better electron donor than the free N–H in the ICT transition. The large red shift observed ($\Delta\lambda_{ICT}$ = 49–74 nm) may be due to the attachment of the receptor unit (N–H) directly to the signalling unit (quinone).

Practical application

An easy-to-use test paper was developed for the instant sensing of fluoride and cyanide ions as their sodium salts in aqueous solution. A paste of **2f** in DMSO was coated on a Whatman paper strip and dried in air. The pale yellow colored strip thus obtained was dipped in an aqueous solutions of NaF or NaCN of varying concentrations. As shown in Fig. 9, color changes of

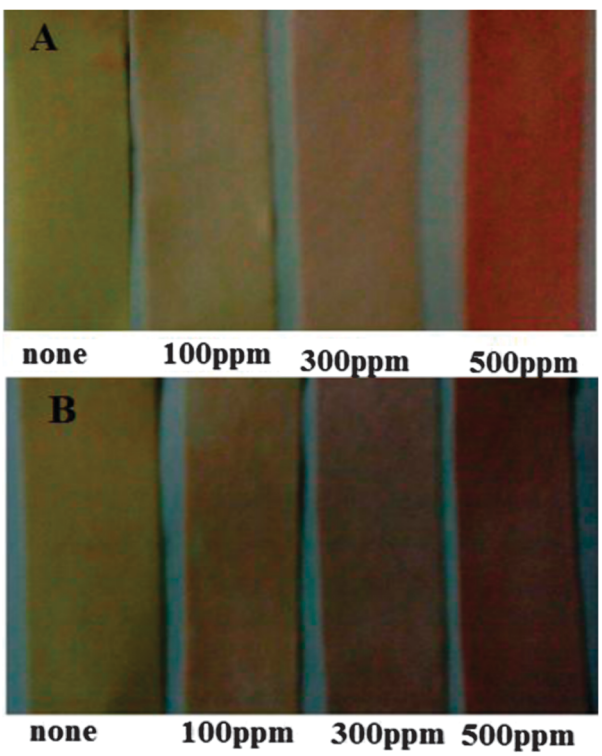

Fig. 9 Color changes of the test papers (coated with **2f**) for detecting (A) F^-, (B) CN^-, in aqueous solution with different concentrations.

the test papers can be observed for the aqueous solutions containing F^- and CN^- ions. We hope that this kind of less expensive and effective new receptor will prove advantageous in sensing these anions in real life applications.

Conclusions

In conclusion, we have synthesized eight new imidazole functionalized receptors wherein the acidity of the imidazole H-atom (N–H) can significantly be enhanced by attaching it directly to an electron deficient quinone moiety. Also, the acidity can be tuned by varying the substituent (R) present on the imidazole moiety. The receptor with an isopropyl substituent exhibited the lowest and that with a thiophene substituent showed the highest δ_H for the H-atom. Such a H-atom, with an enhanced H-bond donor ability, easily forms a 1:1 complex with fluoride and cyanide ions, which exhibit an obvious color change for naked-eye detection. The receptors showed no color change with other anions like Cl^-, Br^-, I^-, NO_3^-, AcO^- and $H_2PO_4^-$. Various spectral techniques such as UV-Vis, fluorescence, ^{1}H NMR and electrochemical studies were employed to investigate the mechanism of the sensing event. The results of the theoretical calculation matches well with the observed electronic spectral behavior of these receptors. The receptor with the thiophene substituent was found to exhibit the same color change in aqueous medium when in the presence of sodium fluoride and sodium cyanide.

Experimental section

Chemicals and apparatus

All the reagents used for synthesis of the receptors were obtained commercially (Aldrich, India) and were used without further purification. Spectroscopic grade solvents (Merck, India) were used as received. UV-Vis spectral studies (V 630 JASCO, Japan) were carried out in DMSO (or) DMSO–water (1:1 v/v). Steady state fluorescence spectra were obtained on a spectrofluorometer (JASCO 6200 Japan). The excitation and emission slit width (5 nm) and the scan rate (250 mV s^{-1}) were kept constant for all of the experiments. Nuclear magnetic resonance spectra were recorded in DMSO-d_6 (Bruker, ^{1}H NMR 300 MHz, ^{13}C NMR 75 MHz). The ^{1}H-NMR spectra data is expressed in the form: chemical shift in units of ppm (normalized integration, multiplicity, and the value of J in Hz). The ^{13}C NMR spectra of the compounds, except **2b** and **2g**, were not recorded due to their low solubility. The differential pulse voltammetric (DPV) experiments, of 1 mmol solutions of the compounds, were carried out using GC as working, Pt wire as reference and Ag wire as auxiliary electrodes in DMSO containing 0.1 M tetrabutylammonium perchlorate electrolyte at a scan rate of 100 mV s^{-1}. The electrochemical measurements were carried out with CHI electrochemical workstation (Model 643B, Austin, TX, USA).

Synthesis and characterization of 1[49]

To a stirred solution of 2,3-dichloro-1,4-naphthoquinone (20 g, 0.09 mol) in ACN (400 mL) potassium phthalimide (19.66 g, 0.1 mol) was added. The reaction mixture was refluxed for 12 h under a nitrogen atmosphere. Afterwards the reaction mixture was cooled to RT and filtered through filter paper, the residue was then washed with water (300 mL). The yellow solid obtained was dried under vacuum. The fine yellow solid was transferred to a 1 L round bottom flask containing 500 mL of distilled water, to which 100 mL of hydrazine hydrate (90%) was added. The reaction mixture was heated to 60 °C for 12 h. Finally the reaction mixture was cooled to RT and then filtered through a filter paper and washed with water to obtain the pure product (**1**) as a dark blue powder (12 g, yield = 72%).

^{1}H NMR (300 MHz, DMSO-d_6) δ_{ppm}: 5.46 (s, 4H), 7.57–7.61 (m, 2H), 7.74–7.77 (m, 2H).

General procedure for synthesis of (2a–2h)[50]

A mixture of compound **1** (0.5 g, 2.65 mmol) and the corresponding aldehyde (2.65 mmol) in DMSO (5 mL) was heated at 90 °C with stirring for 6 h. After cooling to room temperature, the precipitate obtained was filtered from the reaction mixture using filter paper and was washed with cold ethanol to obtain the pure product. The products were characterized using ^{1}H and ^{13}C NMR and LC-MS techniques. The results are:

2-Phenyl-1*H*-naphtho[2,3-*d*]imidazole-4,9-dione (2a)

δ_H (300 MHz; DMSO-d_6; Me_4Si): 7.29 (s, 1H), 7.54 (d, 2H, J = 7.2 Hz), 7.84–7.87 (m, 2H), 8.10–8.13 (m, 2H), 8.23–8.26 (m, 2H), 14.37 (s, 1H).

LCMS (ESI-APCI) m/z: $[M + H]^+$ calcd for $C_{17}H_{10}N_2O_2H$, 275.0, found, 275.0.

2-(Naphthalen-1-yl)-1*H*-naphtho[2,3-*d*]imidazole-4,9-dione (2b)

δ_H (300 MHz; DMSO-d_6; Me_4Si): 7.59–7.69 (m, 3H), 7.84–7.87 (m, 2H), 8.03–8.15 (m, 5H), 8.93 (d, 2H, J = 8.1 Hz).

δ_C (75 MHz; DMSO-d_6; Me_4Si): 125.1, 126.1, 126.2, 126.3, 126.4, 127.0, 128.3, 128.4, 130.3, 130.5, 132.9, 133.4, 133.6, 139.7, 153.4, 177,1, 181.2.

LCMS (ESI-APCI) m/z: $[M + H]^+$ calcd for $C_{21}H_{12}N_2O_2H$, 325.0, found, 325.0.

2-(4-Nitrophenyl)-1*H*-naphtho[2,3-*d*]imidazole-4,9-dione (2c)

δ_H (300 MHz; DMSO-d_6; Me_4Si): 7.83–7.86 (m, 2H), 8.09–8.12 (m, 2H), 8.39 (d, 2H, J = 8.7 Hz), 8.49 (d, 2H, J = 9 Hz), 14.89 (s, 1H).

LCMS (ESI-APCI) m/z: $[M + H]^+$ calcd for $C_{17}H_9N_3O_4H$ $(M + H)^+$, 320.0, found, 320.0.

2-(3-Phenoxyphenyl)-1*H*-naphtho[2,3-*d*]imidazole-4,9-dione (2d)

δ_H (300 MHz; DMSO-d_6; Me_4Si): 7.13 (t, 2H, J = 8.4 Hz), 7.23–7.17 (m, 2H), 7.48 (t, 2H, J = 8.4 Hz), 7.59 (t, 1H, J = 8.1 Hz), 7.83–7.87 (m, 3H), 8.03 (d, 1H, J = 7.8 Hz), 8.07–8.10 (m, 2H), 14.39 (s, 1H).

LCMS (ESI-APCI) m/z: $[M + H]^+$ calcd for $C_{23}H_{14}N_2O_3H$, 367.0, found, 367.0.

2-(Pyridin-2-yl)-1*H*-naphtho[2,3-*d*]imidazole-4,9-dione (2e)

δ_H (300 MHz; DMSO-d_6; Me_4Si): 7.55–7.59 (m, 1H), 7.85–7.88 (m, 2H), 8.01–8.07 (m, 1H), 8.10–8.13 (m, 2H), 8.3 (d, 1H, J = 8.1 Hz), 8.76 (d, 1H, J = 4.2 Hz), 14.62 (s, 1H).

LCMS (ESI-APCI) m/z: $[M + H]^+$ calcd for $C_{16}H_9N_3O_2H$, 276.0, found, 276.1.

2-(Thiophen-2-yl)-1*H*-naphtho[2,3-*d*]imidazole-4,9-dione (2f)

δ_H (300 MHz; DMSO-d_6; Me_4Si): 7.23–7.26 (m, 1H), 7.80–7.86 (m, 3H), 8.02 (d, 1H, J = 3.6 Hz), 8.08–8.11 (m, 2H), 14.94 (s, 1H).

LCMS (ESI-APCI) m/z: calcd for $C_{15}H_8N_2O_2S$ $(M - H)^-$, 280.0, found, 278.9.

2-Isopropyl-1*H*-naphtho[2,3-*d*]imidazole-4,9-dione (2g)

δ_H (300 MHz; DMSO-d_6; Me_4Si): 1.33 (d, 6H, J = 7.2 Hz), 3.06–3.20 (m, 1H), 7.81–7.84 (m, 2H), 8.05–8.08 (m, 2H), 13.70 (s, 1H).

δ_C (75 MHz; DMSO-d_6; Me_4Si): 22.0, 33.2, 125.2, 126.1, 126.3, 126.8, 130.7, 131.0, 133.3, 133.8, 135.5, 142.8, 177.3, 181.1. LCMS (ESI-APCI) m/z: calcd for $C_{14}H_{12}N_2O_2H$ $(M + H)^+$, 241.0, found, 241.0.

2-(Trifluoromethyl)-1*H*-naphtho[2,3-*d*]imidazole-4,9-dione (2h)

δ_H (300 MHz; DMSO-d_6; Me_4Si): 7.83–7.86 (m, 2H), 8.08–8.11 (m, 2H).

LCMS (ESI-APCI) m/z: calcd for $C_{12}H_5F_3N_2O_2$ $(M - H)^-$, 266.0, found, 265.0.

Acknowledgements

The authors thank the Council of Scientific and Industrial Research, New Delhi, for the financial assistance to carry out this work [02(0118)/13/EMR II].

References

1 M. P. Anderson, R. J. Gregory, S. Thompson, D. W. Souza, S. Paul, R. C. Mulligan, A. E. Smith and M. J. Welsh, *Science*, 1991, **253**, 202–205.
2 M. Kleerekoper, *Endocrinol. Metab. Clin. North Am.*, 1998, **27**, 441–452.
3 B. Schwartz and D. G. Drueckhammer, *J. Am. Chem. Soc.*, 1995, **117**, 11902–11905.
4 J. F. Clark, D. L. Clark, G. D. Whitener, N. C. Schroeder and S. H. Straus, *Environ. Sci. Technol.*, 1996, **30**, 3124–3126.
5 K. J. Wallace, Y. C. Yang, J. A. Barker and J. R. Ward, *Chem. Rev.*, 1992, **92**, 1729–1743.
6 K. J. Wallace, R. I. Ragmemi, F. J. Folmer-Anderson, J. Morey, V. M. Lynth and E. V. Anslyn, *Chem. Commun.*, 2006, 3886–3888.
7 T. J. Dale and J. Rebek, *J. Am. Chem. Soc.*, 2006, **128**, 4500–4501.
8 *Guideline for Drinking water Quality*, World Health Organization, Geneva, 1993.
9 *Guideline for Drinking water Quality*, World Health Organization, Geneva, 1996.
10 H. Komatsu, T. Miki, D. Citterio, T. Kubota, Y. Shindo, Y. Kitamura, K. Oka and K. Suzuki, *J. Am. Chem. Soc.*, 2005, **127**, 10798–10799.
11 N. Kaur and S. Kumar, *Chem. Commun.*, 2007, 3069–3070.
12 M. Schmittel and H. W. Lin, *Angew. Chem., Int. Ed.*, 2007, **46**, 893–896.
13 C. Lee, D. H. Hong and J. I. Hong, *Tetrahedron Lett.*, 2001, **42**, 8665–8668.
14 A. Satheshkumar and K. P. Elango, *Dyes Pigm.*, 2013, **96**, 364–371.
15 D. A. Jose, A. Singh, A. Das and B. Ganguly, *Tetrahedron Lett.*, 2007, **48**, 3695–3698.
16 L. S. Evans, P. A. Gale, M. E. Light and R. Qyesada, *Chem. Commun.*, 2006, 965–967.
17 T. Mizuno, W.-H. Wei, L. R. Eller and J. L. Sessler, *J. Am. Chem. Soc.*, 2002, **124**, 1134–1135.
18 J. You, H. Jeong, H. Seo and S. Jeon, *Sens. Actuators, B*, 2010, **146**, 160–164.
19 J. L. Sessler, D. Cho and V. Lynch, *J. Am. Chem. Soc.*, 2006, **128**, 16518–16519.
20 K. Chang, D. Moon, M. S. Lah and K.-s. Jeong, *Angew. Chem.*, 2005, **117**, 8140–8143.
21 F. Zapata, A. Caballero, A. Espinosa, A. Tarrage and P. Molina, *J. Org. Chem.*, 2008, **73**, 4034–4044.
22 X. Peng, Y. Wu, J. Fan, M. Tian and K. Han, *J. Org. Chem.*, 2005, **70**, 10524–10531.
23 H. Miyaji, W. Sato and J. L. Sessler, *Angew. Chem., Int. Ed.*, 2000, **39**, 1777–1780.
24 A. J. Evans, S. E. Mathews, A. R. Cowley and P. D. Beer, *Dalton Trans.*, 2003, 4644–4650.
25 Z. Lin, Y. Zhao, C. Duan, B. Zhanga and Z. Bai, *Dalton Trans.*, 2006, 3678–3684.
26 Q. Li, Y. Guo, J. Xu and S. Shao, *J. Photochem. Photobiol., B*, 2011, **103**, 140–144.
27 E. J. Cho, H. M. Yeo, B. J. Ryu, H. A. Jeong and K. C. Nam, *Bull. Korean Chem. Soc.*, 2006, **27**, 1967–1968.
28 P. Anzenbacher, M. A. Palacios, K. Jursikova and M. Marquez, *Org. Lett.*, 2005, **7**, 5027–5030.
29 G. J. Mohr, *Chem. Commun.*, 2002, 2248.
30 S. Park, K.-H. Hong, J.-I. Hong and H.-J. Kim, *Sens. Actuators, B*, 2012, **174**, 140–144.
31 K.-H. Hong and H.-J. Kim, *Supramol. Chem.*, 2013, **25**, 24–27.
32 A. Satheshkumar and K. P. Elango, *RSC Adv.*, 2013, **3**, 1502–1508.
33 T. N. Brown and N. Mora-Diez, *J. Phys. Chem. B*, 2006, **110**, 9270–9279.
34 V. Kumar, M. P. Kaushik, A. K. Srivastava, A. Pratap, V. Thiruvenkatam and T. N. Gururow, *Anal. Chim. Acta*, 2010, **663**, 77–84.
35 K.-S. Lee, H.-J. Kim, G.-H. Kim, I. Shin and J.-I. Hong, *Org. Lett.*, 2008, **10**, 49–51.
36 J. H. Lee, A. R. Jeong, I.-S. Shin, H.-J. Kim and J.-I. Hong, *Org. Lett.*, 2010, **12**, 764–767.
37 S. Park and H.-J. Kim, *Chem. Commun.*, 2010, **46**, 9197–9199.
38 H. Lee and H.-J. Kim, *Tetrahedron Lett.*, 2012, **53**, 5455–5457.
39 S. Park and H.-J. Kim, *Sens. Actuators, B*, 2012, **161**, 317–321.

40 S. Goswami, A. Manna, S. Paul, A. K. Das, K. Aich and P. K. Nandi, *Chem. Commun.*, 2013, **49**, 2912–2914.
41 S. Goswami, A. Manna, S. Paul, K. Aich, A. K. Das and S. Chakraborty, *Tetrahedron Lett.*, 2013, **54**, 1785–1789.
42 J. Shao, Y. Wang, H. Lin, J. Li and H. Lin, *Sens. Actuators, B*, 2008, **134**, 849–853.
43 R. L. Scott, *Recl. Trav. Chim. Pays-Bas Belg.*, 1956, **75**, 787–789.
44 F. Ding, G. Zhao, J. Huang, S. Ying and Z. Li, *Eur. J. Med. Chem.*, 2009, **44**, 4083–4089.
45 K. K. Upadhyay, R. K. Mishra, V. Kumar and P. K. RoyChowdhury, *Talanta*, 2010, **82**, 312–318.
46 T. Ghosh, B. G. Maiya and M. W. Wong, *J. Phys. Chem. A*, 2004, **108**, 11249–11259.
47 V. A. Nikitina, R. R. Nazmutdinov and G. A. Tsirlina, *J. Phys. Chem. B*, 2011, **115**, 668–677.
48 M. J. Frisch, G. W. Trucks, H. B. Schlegel, G. E. Scuseria, M. A. Robb, J. R. Cheeseman, J. A. Jr., Montgomery, T. Vreven, K. N. Kudin, J. C. Burant, J. M. Millam, S. S. Iyengar, J. Tomasi, V. Barone, B. Mennucci, M. Cossi, G. Scalmani, N. Rega, G. A. Petersson, H. Nakatsuji, M. Hada, M. Ehara, K. Toyota, R. Fukuda, J. Hasegawa, M. Ishida, T. Nakajima, Y. Honda, O. Kitao, H. Nakai, M. Klene, X. Li, J. E. Knox, H. P. Hratchian, J. B. Cross, V. Bakken, C. Adamo, J. Jaramillo, R. Gomperts, R. E. Stratmann, O. Yazyev, A. J. Austin, R. Cammi, C. Pomelli, J. W. Ochterski, P. Y. Ayala, K. Morokuma, G. A. Voth, P. Salvador, J. J. Dannenberg, V. G. Zakrzewski, S. Dapprich, A. D. Daniels, M. C. Strain, O. Farkas, D. K. Malick, A. D. Rabuck, K. Raghavachari, J. B. Foresman, J. V. Ortiz, Q. Cui, A. G. Baboul, S. Clifford, J. Cioslowski, B. B. Stefanov, G. Liu, A. Liashenko, P. Piskorz, I. Komaromi, R. L. Martin, D. J. Fox, T. Keith, M. A. Al-Laham, C. Y. Peng, A. Nanayakkara, M. Challacombe, P. M. W. Gill, B. Johnson, W. Chen, M. W. Wong, C. Gonzalez and J. A. Pople, *Gaussian, 03, Revision D.01*, Gaussian, Inc., Wallingford CT, 2004.
49 R. Diaz, O. Reyes, A. Francois, A. M. Leiva and B. Loeb, *Tetrahedron Lett.*, 2001, **42**, 6463–6467.
50 A. A. Aly, A. A. Hassan, A. B. Brown, K. M. El-Shaieb and T. M. I. Bedair, *J. Heterocycl. Chem.*, 2011, **48**, 787–791.